18th International Conference on Renewable Energies and Power Quality (ICREPQ'20)
Granada (Spain), 1st to 2nd April 2020
Renewable Energy and Power Quality Journal (RE&PQJ)
ISSN 2172-038 X, Volume No.18, June 2020

Heliostat Dual-Axis Sun Tracking System: A Case Study in KSA

W. M. Hamanah[1,2], A. Salem[1], and M. A. Abido[1,2]

1. Department of Electrical Engineering, King Fahd University for Petroleum and Minerals, Dhahran, 31261, KSA
2. K.A.CARE Energy Research & Innovation Center, King Fahd University for Petroleum and Minerals, Dhahran, KSA

Fax number: +966-3-8603535,

e-mail: **g201105910@kfupm.edu.sa**, **asalem@kfupm.edu.sa**, **mabido@kfupm.edu.sa**

Abstract. This paper demonstrates a case study for solar power tower (SPT) Heliostat, concentrated solar power topology in Dhahran, KSA. A MATLAB code is implemented for the solar position algorithm to calculate the incident angles in order to track the sunbeams during the whole year. A drive system composed of two linear actuators; DC motor-based drive is developed. The model has been validated experimentally using a rooftop Heliostat prototype. The experimental platform has been tested for several days in different seasons to confirm the prototype capabilities for sun tracking during the whole year. The experimental and simulation results are well agreed.

Key words. Sun tracking system, Heliostat, DC motor.

1. Introduction

Nowadays, most researchers focus on renewable energy resources as potential alternatives to fossil fuel to reduce CO_2 emissions and to obtain a clean environment. One of the most important energy sources on earth is the sun. A huge amount of solar energy is received to earth every day. The scientists classify the sunrays arriving earth into different categories. There are direct, reflected, and scattered radiations. These categories can be used in different technologies to use efficiently the energy received from the sun. There are four different well-known topologies for the concentrated solar power (CSP) [1]-[4]. Solar Power Tower (SPT) is a promising technology compared to the other different topologies where it is characterized by higher efficiency and temperatures. Frankly speaking, the efficiency of SPT depends on the ability of the Heliostats to reflect the sunbeams onto the receiver accurately. It requires an accurate drive system to move the Heliostat over a wide range of angles, which represents a challenge in the development of new efficient and low-cost drive system designs.

Different types of dual-axis solar tracking systems were illustrated in [5]. It has been concluded that the dual-axis solar tracking system, which depends on azimuth/elevation control, was the most efficient approach. A brief description for azimuth and elevation angles solar tracking system was provided in [6], where several corrections to describe angles, as well as methods of integrating the data into a Geographic Information System (GIS) are presented. A mathematical modulation method was involved in [7], and it used to define the parameters which must be provided by solar azimuthal and elevation angles to guide a small scale Heliostat. The analyzes tracking system of the elevation and azimuth tracking formulas were studied in [8]. With negligible tracking error, formulas were used to get the accurate results. Actual Heliostat units in a field was used to demonstrate the use of the general tracking formulas, with both tracking elevation and azimuth angles. The dual-axis sun tracking system program had developed and simulated in Algeria using Proteus software in [9]. The study used two DC motors to move the unit in two directions to track the sun path. They provided the distinction between day and night with the light-dependent resistor (LDR). The optimal design of a Heliostat unit for a SPT was studied with a control system in real-time in [10]. The study used an illuminance sensor to track sun positions. Optimized algorithms were applied to maximize the efficiency of the solar system. Dynamic models were presented to describe the behavior of the overall system for the mechanical and control components in [11]. Based on modeling and simulation, the models involved the system parameters, as the motor parameters, power screw, Heliostat mass, load forces, and wind forces. A based-PID tracking control is used for the solar tracking. A 3D CAD models are developed to simulate the integrated system. The methodology was presented to employ the design of the Heliostat unit with a small mirror size of 3 m^2. The angular parametric properties of the dual-axis tracking angles were discussed in [12]. An approach was provided to evaluate the accuracy of tracking angles using experimental solar tracking data. It has been observed that the azimuth and elevation solar racking angles are more useful and effective in the design of the dual-axis solar tracking system. The active solar tracking system was provided in [13]. The solar position was calculated using A micro-controller that was designed automatically catch the solar position. Two motors were used to calibration tests and a Heliostat tracking positioning test with two micro switches, with decreasing the costs and increasing the accuracy. Using the Arduino platform and C programming language a highly efficient two-axis solar tracking system was designed and developed in [14]. The work divided into parts hardware and software development. Five LDRs had been used for capturing maximum light source with two servomotors that have been used to move the panel. Several time intervals were used to compare the efficiency of the system. A laboratory prototype for solar tracking system was created and developed in [15]. The system was applied under a fixed solar system and then it was converted to a polar-axis tracking system. The study is performed on a PV module to Maximum Power Point Tracking (MPPT), and they compared the results with an old fixed system. The results were indicated that ensures the MPPT has energy-efficient and more reliability than a modified fixed solar panel.

In this paper, a solar drive system with dual-axis tracking has been developed and simulated for the site of Dhahran, in the east of KSA. A MATLAB code is implemented to simulate solar and Heliostat azimuth and elevation angles for the whole year. Arduino microcontroller is interfaced to global position sensor (GPS) to extract the time and location. Then, Heliostat angles are calculated in order to move the dual axis drive systems. The proper switching pulses are generated to steer the power electronic converter for the accurate movement.

This paper is organized as follows: in Section 2, the proposed tracking system components are involved, and the modelling and analysis of dual-axis tracking system is provided. The mathematical model simulation results applied to Dhahran, KSA is presented and discussed in Section 3. Then, Section 4 presents the drive system experimental setup. An integrated Heliostat prototype is explained and presented in Section 5. Finally, a conclusion is derived in Section 6.

2. Modelling and Analysis of Dual-Axis Tracking System

The solar tracking systems must be adjusted continually accurately to collect the sunbeams. A single-axis tracking system is less costly, and its control system is simple to achieve. However, their efficiency is less compared with the dual-axis solar tracking system. Fig. 1 shows the basic components of the proposed tracking system. It consists of a power electronics converter connected to an electric motor, which is coupled to the linear actuator. Position sensor is used to feedback the motor position to control accurately the motor position of the drive system. The sun-tracking algorithm is implemented within the control unit to deliver the control pulses to the power electronic converter and moving the actuators to the targeted angles.

To track the sunbeams, three sets of angles have to be defined, i.e. sun, tower and Heliostat angles. The following subsection describes the mathematical model used to define these angles.

A. Solar Sun Model

Sun position is defined by two principal's angles, solar altitude angle (αs) and solar azimuth angle (γs), where sun vector is defined by declination angle (δ) and the time angle (ω).

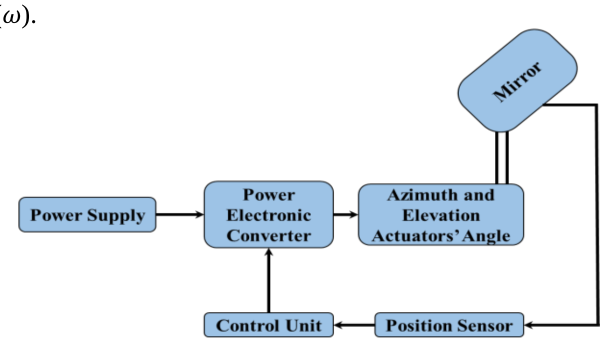

Fig. 1: Schematic diagram for the basic solar tracking system

The declination angle, that is used to calculate on any given day, is described by [6],[7]:

$$\delta = 23.45 \sin\left(360 \times \frac{284 + n}{365}\right) \qquad (1)$$

where, δ is declination angle, and n is the day number; such that n = 1 on the 1st January.

Depending on time and date values (year, month, day, hour, min, and sec), and location (longitude (φ) and latitude angles), the solar altitude and azimuth angles are described in Fig. 2. The solar vector algorithm is used for its simplicity and they are calculated by [6],[7]:

$$\alpha_s = \sin^{-1}\left[\cos(\varphi)\cos(\delta)\cos(\omega) + \sin(\varphi)\sin(\delta)\right]$$
$$\gamma_s = sign(\omega)\left|cos^{-1}\left(\frac{\cos(\theta_z)\sin(\varphi) - \sin(\delta)}{\sin(\theta_z)\cos(\varphi)}\right)\right| \qquad (2)$$

B. Tower and Heliostat Model

The solar altitude angle of the target receiver for each Heliostat (α_T) which is defined by the tower height *(H)*, the height of each Heliostat (*h*) and the distance of Heliostat from the tower base *(R)* are illustrated in Fig. 3. The target position of solar tower also is defined by the azimuth target angle (γ_T) which is a relationship with the North direction at a Heliostat and tower.

Some preliminary works have been done on Heliostat angles for elevation and azimuth angles. Two Heliostat angles are called mirror angles. Fig. 4 shows both elevation and azimuth mirror angles. The model converts the sun and tower angles to points and then find the normal mirror vector based on three-dimensional Cartesian form (x, y, & z).

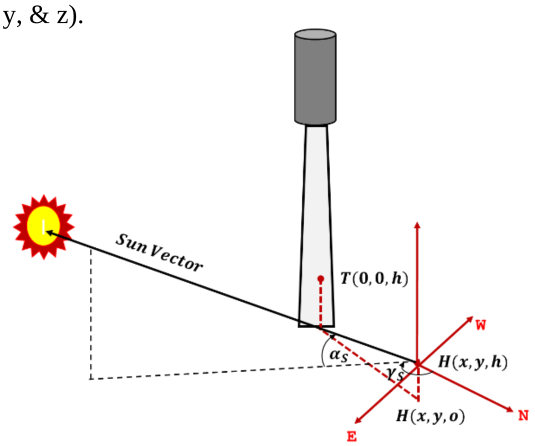

Fig. 2. Elevation and azimuth sun angles

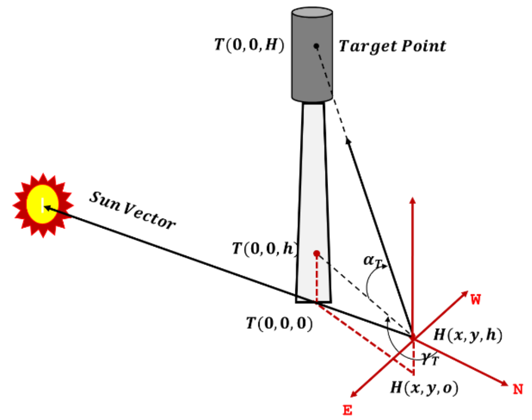

Fig. 3. Elevation and azimuth target angles

The following is the mathematical expressions for the solar tracking system used to calculate both Heliostat angles [8]:

- Convert the two sun angles to x_1, y_1, & z_1 values

$$\begin{aligned} z_1 &= \sin(\alpha_S) \\ hyp &= \cos(\alpha_S) \\ x_1 &= hyp * \cos(\gamma_S) * -1 \\ y_1 &= hyp * \sin(\gamma_S * -1) \end{aligned} \tag{3}$$

- Convert the two target angles to x_2, y_2, & z_2 values:

$$\begin{aligned} z_2 &= \sin(\alpha_T) \\ hyp &= \cos(\alpha_T) \\ x_2 &= hyp * \cos(\gamma_T) * -1 \\ y_2 &= hyp * \sin(\gamma_T * -1) \end{aligned} \tag{4}$$

- From both points, x, y, and z are calculated:

$$\begin{aligned} x &= \frac{x_1 - x_2}{2} + x_2 \\ y &= \frac{y_1 - y_2}{2} + y_2 \\ z &= \frac{z_1 - z_2}{2} + z_2 \end{aligned} \tag{5}$$

$$\begin{aligned} distance &= \sqrt{x^2 + y^2 + z^2} \\ \alpha_H &= asin\left(\frac{z}{distance}\right) \\ \gamma_H &= atan2(y * -1, x) \end{aligned} \tag{6}$$

3. Simulation of Dual-Axis Tracking System

Solar angles for typical days (1st day of each month in 2019) are simulated based on the longitude of the AL Dhahran KSA solar field is longitude (φ= 50.01°) and the latitude is 26.5. The solar altitude angle, (α_S), and the solar azimuth angle, (γ_S), are calculated using (2), and plotted for twelve typical days as illustrated in Fig. 5 and Fig. 6 where "$\alpha_s = Jan.$" means the solar altitude angle for the 1st January with the other symbols referring to the other dates. In addition, "$\gamma_s = Jan.$" means the solar azimuth angle for the January first with the other symbols referring to the other dates.

Simulated tracking angles from the altitude–azimuth tracking formulas considered the Heliostat position from tower, with $\boldsymbol{\alpha_T = 38.71° \; and \; \gamma_T = 170.77°}$. The sun and Heliostat angles are illustrated in Fig. 5-Fig. 8. These figures reflect the long sunny day in this location, which is a promising location for CSP applications.

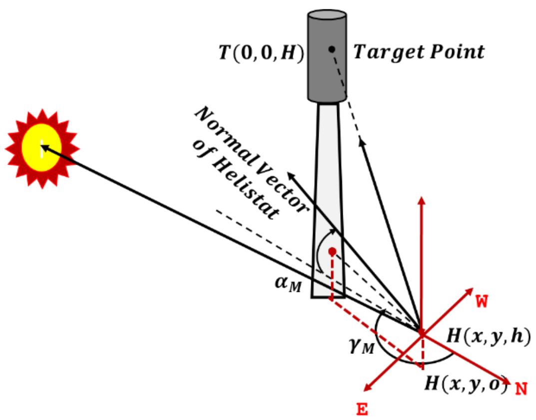

Fig. 4. Elevation and azimuth Heliostat angles

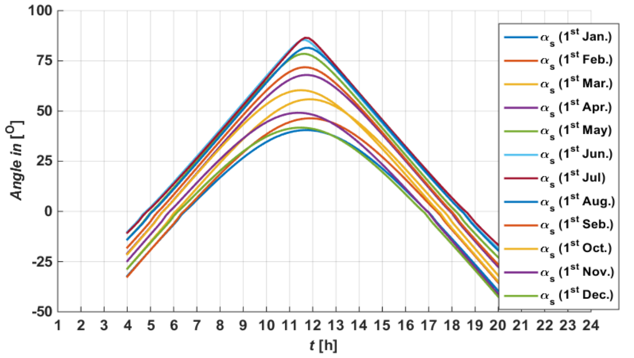

Fig. 5. Solar angle curves with respect to Dhahran time, the solar altitude angle, $\boldsymbol{\alpha_s}$, from Eq. (2)

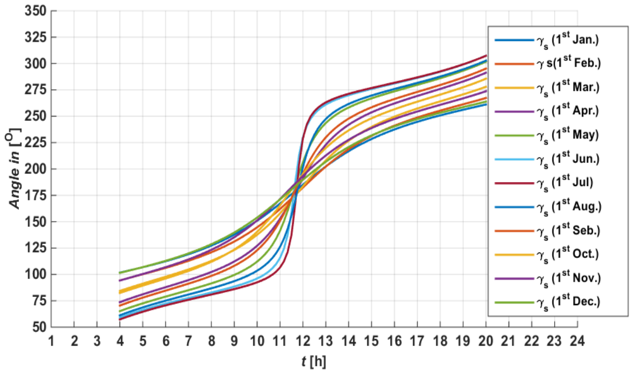

Fig. 6. Solar angle curves with respect to Dhahran time, the solar azimuth angle, $\boldsymbol{\gamma_s}$, from Eq. (2)

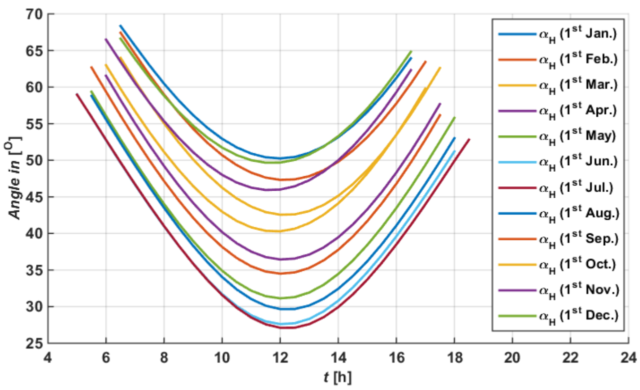

Fig. 7. Heliostat angle curves with respect to Dhahran time, the Heliostat altitude angle, $\boldsymbol{\alpha_H}$, from Eq. (6)

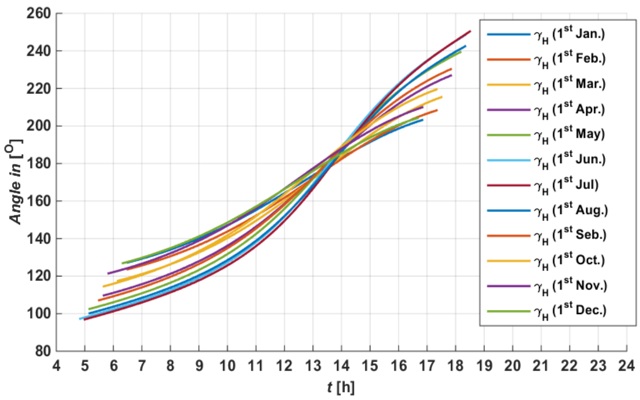

Fig. 8. Heliostat angle curves with respect to Dhahran time, the Heliostat azimuth angle, $\boldsymbol{\gamma_H}$, from Eq. (6)

4. Heliostat Prototype

A Heliostat prototype of an adequate scale is implemented in the Dhahran area, KSA, to the theoretical study. A block diagram for the dual axes Heliostat is shown in Fig. 9. It consists of dual DC drive systems; i.e. elevation and azimuth drives. Each drive system consists of linear actuator based on a permanent magnet (PMDC) motor supplied from a class-E four-quadrant DC chopper. This drive system is preferred to steer the motor in forward and reverse directions. In additions, it gives the opportunity to operate at the four quadrant modes that may occurred during speed control. The two drive systems are interfaced to Arduino-Uno digital controller that provides the proper pulses to the different drive systems. A position sensor is used to provide the actual position of the mirror in terms of elevation and azimuth angles. Then, the measured angles are compared to the reference angles that is calculated by the digital controller as a function of the time and location given by a global positioning system (GPS) sensor. Then, the PI controller is used to minimise the angles errors and provide the proper duty cycle. After that, the duty signal is modulated at a reasonable switching frequency to steer the semiconductor switches by the proper pulses. A picture for the preliminary DC drive system prototype is shown in Fig. 10. The complete integrated Heliostat prototype is shown in Fig. 11-a. The location is a rooftop of an academic building in King Fahd University in Dhahran, KSA. Fig. 11-b declares the Heliostat operation at one instant while the mirror could reflect the sunbeams to the desired target. The corresponding drive system results and the drive system response will be discussed in the next section.

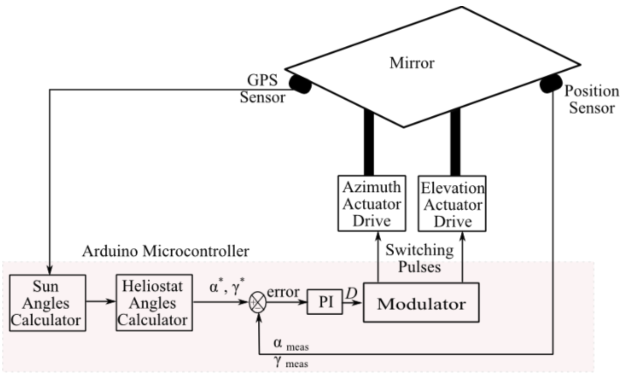

Fig. 9. Block diagram of dual-axis solar tracking system

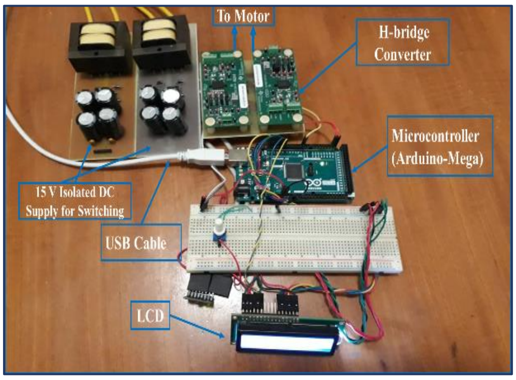

Fig. 10. Experimental setup for a four-quadrant DC-chopper

(a) (b)

Fig. 11. The proposed prototype of the automatic dual-axis solar tracking unit.

5. Experimental Results

The proposed drive system has been tested based on the field dimensions and coordinates listed in Appendix-A. The machine current, voltage and the Arduino control pulses are shown in Fig. 12 for forward and reverse motoring modes. The switching frequency of the control pulses is adjusted to 4 kHz, which is suitable for the DC drives application. The spikes at the on- and off-transitions is a result of the high switching frequency and the low gate resistor of the driving circuit used.

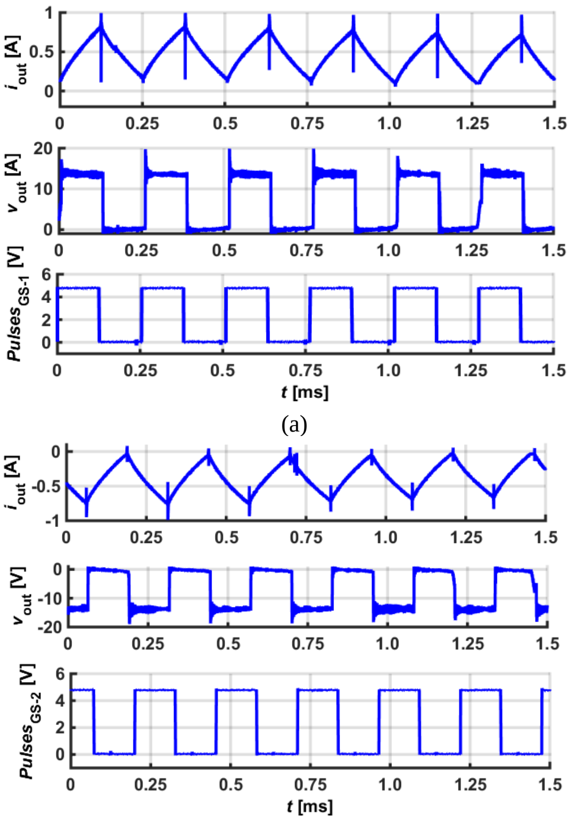

(b)

Fig. 12. Motor current, voltage and MOSFET gate-source pulses for (a) forward mode and (b) reverse mode.

An experiment has been conducted for several days to show the drive system performance at several conditions. Due to the paper length limitation, only one complete day (Sept. 10th, 2019) from sunrise to sunset is presented here.

However, the drive system could reflect the sunbeams accurately similar to the presented one-day results. A step-time is designated to be 30 minutes between each two successive motions. This time may not be the optimum time for this drive system. However, it has been assumed here just to test the drive system performance. The optimal step-time will be considered in future work.

The operation of the proposed system is described as follows. Firstly, the Heliostat started its operation from the stow-position, which is shown in Fig. **11**-a. The sunrise time at Dhahran at the day of test was 6.30 AM. Therefore, the drive system start the motion from the stow-position to the calculated heliostat angles at very small time, few seconds, as shown in Fig. 13 for both azimuth and elevation angles. Then, the tracking system could follow the reference Heliostat angles along the day as shown in the same figure. Finally, at the sunset time, which is 5.00 PM in Dhahran, the Heliostat drive returned the mirror to the stow-position. The figure reflects that the drive system could follow the reference angles properly.

The dynamic response of the drive system for one motion, for both azimuth and elevation drives, are demonstrated in Fig. 14.

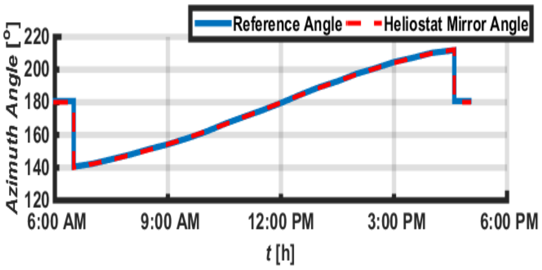

(a)

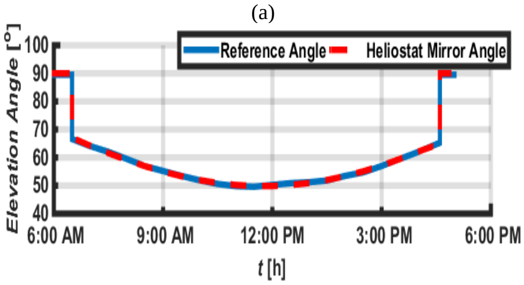

(b)

Fig. 13. (a) Reference and tracking angle for azimuth motion angle. (b) Reference and tracking angle for elevation motion angle with Heliostats mirror angles on 10th. Sep. 2019

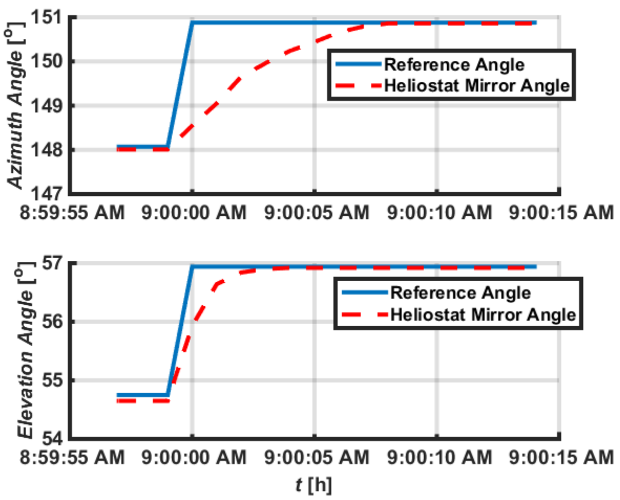

Fig. 14. Reference tracking angles for azimuth and elevation with Heliostats mirror angles at 09:00 AM

The response shows that the drive system could attain the reference angles in a reasonable time and acceptable steady-state errors. Considering the error relation as:

$$\alpha_{err} = \frac{|\alpha^* - \alpha_{meas}|}{\alpha_{base}}$$
$$\gamma_{err} = \frac{|\gamma^* - \gamma_{meas}|}{\gamma_{base}} \quad (7)$$

Where $\alpha_{base} = 70^o$ and $\gamma_{base} = 210^o$, the steady-state errors are found 0.167% and 0.343% for both azimuth and elevation angles, respectively. This reflects how the system is able to reflect the sunbeams accurately.

6. Conclusion

This paper discussed the dual-axis Heliostat solar drive system, a part of a developing renewable energy technology, as a case study in eastern province in KSA. The work discussed the mathematical solar position algorithm used for Heliostat sun tracking system. The mathematical algorithm has been implemented both in simulation using Matlab/Simulink and in experimentally using Arduino Microcontroller. The implemented algorithm could deliver accurate elevation and azimuth tracking angles in both simulation and experiments. The experimental results have been demonstrated for the rooftop Heliostat prototype in KFUPM, Dhahran, KSA. The conducted test and the recorded results reflect the ability of the prototype drive system to reflect accurately the sunbeams to the desired target.

Appendix A

Site, Tower and Heliostat coordinates

Description	Value
Mirror size	1.2×0.7 m^2
Target high	7.48 m
Heliostat high	1.85 m
Distance between Target and Heliostat unit	6.315 m
Heliostat -Target angle with North	37.24°
Azimuth Heliostat angle	142.77°
Elevation Heliostat angle	41.71°

Acknowledgement

The authors gratefully acknowledge the support provided by King Fahd University of Petroleum & Minerals (KFUPM) (Grant No. GTEC1701), Saudi Arabia. The authors acknowledge also the funding support provided by King Abdullah City for Atomic and Renewable Energy (K.A.CARE).

References

[1] T. PavloviA, and I. RadonjiA, "A review of concentrating solar power plants in the world and their potential use in Serbia," ... *Sustain. Energy* ..., vol. 16, no. 6, p. 12, 2012.

[2] R. Leiva-Illanes, R. Escobar, J. M. Cardemil, D.-C. Alarcón-Padilla, J. Uche, and A. Martínez, "Exergy cost assessment of CSP driven multi-generation schemes: Integrating seawater desalination, refrigeration, and process heat plants," *Energy Convers. Manag.*, vol. 179, no. September 2018, pp. 249–269, 2019.

[3] D. Hess, "The empirical probability of integrating CSP and its cost optimal configuration in a low carbon energy system

of EUMENA," *Sol. Energy*, vol. 166, no. October 2017, pp. 267–307, 2018.

[4] M. Mehos, C. Turchi, J. Vidal, M. Wagner, Z. Ma, C. Ho, W. Kolb, C. Andraka, M. Mehos, C. Turchi, J. Vidal, M. Wagner, Z. Ma, C. Ho, W. Kolb, C. Andraka, A. Kruizenga, and NREL, "Concentrating Solar Power Gen3 Demonstration Roadmap," *NREL Tech. Rep.*, no. January, pp. 1–140, 2017.

[5] H. Mousazadeh, A. Keyhani, A. Javadi, H. Mobli, K. Abrinia, and A. Sharifi, "A review of principle and sun-tracking methods for maximizing solar systems output," *Renew. Sustain. Energy Rev.*, vol. 13, pp. 1800–1818, 2009.

[6] M. L. Roderick, "Methods for Calculating Solar Position and Day Length including computer programs and subroutines," *Dep. Agric. Food, West. Aust.*, no. 137, p. 81, 1992.

[7] M. Debbache *et al.*, "Mathematical modelization of an azimuthal - elevation tracking system of small scale heliostat," *Int. J. Control Theory Appl. ·*, vol. 9, no. 38, pp. 111–120, 2016.

[8] M. Guo, Z. Wang, J. Zhang, F. Sun, and X. Zhang, "Accurate altitude – azimuth tracking angle formulas for a heliostat with mirror – pivot offset and other fixed geometrical errors," *Sol. Energy*, vol. 85, no. 5, pp. 1091–1100, 2011.

[9] M. Sofiane and A. Chermitti, "Two Axes Sun Tracking System for Heliostat : Case Study in Algeria Two Axes Sun Tracking System for Heliostat in Algeria," *Indones. J. Electr. Eng. Informatics*, no. March 2016, 2018.

[10] D. Il Lee, W. J. Jeon, S. W. Baek, and N. T. Ali, "Optimal Design and Control of Heliostat for Solar Power Generation," *IACSIT Int. J. Eng. Technol.*, vol. 4, No. 4, no. January, 2016.

[11] M. A. Rady, A. M. A. Amin, R. H. A. El-hamid, M. M. Nageb, and D. Olasolo, "An Integrated Design Approach of Local Control System of a Linear Drive Single facet Heliostat," in *Proceedings of the ASME 2016 Power Conference*, 2016, no. June 26-30, Charlotte, North Carolina.

[12] M. Guo, F. Sun, Z. Wang, and J. Zhang, "ScienceDirect Properties of a general azimuth – elevation tracking angle formula for a heliostat with a mirror-pivot offset and other angular errors," *Sol. Energy*, vol. 96, pp. 159–167, 2013.

[13] A. Dimitrija, N. Koceska, and S. Koceski, "Low-cost Dual-axis System for Solar Tracking," *2014 3rd Mediterr. Conf. Embed. Comput.*, pp. 169–172, 2014.

[14] M. Zolkapli, Z. Othman, A. Manut, and M. A. M. Zulkifli, "High-efficiency dual-axis solar tracking developement using Arduino," *2013 Int. Conf. Technol. Informatics, Manag. Eng. Environ.*, pp. 43–47, 2013.

[15] H. A. E. Salama, "Practical Implementation of Dual Axis Solar Power Tracking System," *2018 Twent. Int. Middle East Power Syst. Conf.*, pp. 446–451, 2018.